

Supporting Information: Electrosorption of hydrogen in Pd-based metallic glass nanofilms

Baran Sarac,^{†,} Tolga Karazehir,^{‡,\$} Marlene Mühlbacher,[§] Baris Kaynak,[#] Christoph Gammer,[†]*

Thomas Schöberl,[†] A. Sezai Sarac,[‡] Jürgen Eckert^{†,\$}

[†] Erich Schmid Institute of Materials Science, Austrian Academy of Sciences, 8700 Leoben, Austria

[‡] Department of Chemistry, Polymer Science and Engineering, Istanbul Technical University, 80626 Istanbul, Turkey

[§] Faculty of Engineering, Department of Energy System Engineering, Adana Science and Technology University, 01250 Saricam, Adana, Turkey

[§] Montanuniversität Leoben, Department Materials Physics, 8700 Leoben, Austria

[#] Montanuniversität Leoben, Department Polymer Science, 8700 Leoben, Austria

EXPERIMENTAL SECTION

Deposition of thin films by PVD. The substrate material, Si(001) with a native oxide layer ($20 \times 7 \text{ mm}^2$, B-doped, resistivity $\rho = 1\text{-}20 \text{ }\Omega\text{-cm}$), was mounted on a rotatable sample holder opposite to the targets with a target-to-substrate distance of 40 mm. Immediately prior to loading them into the vacuum system, the Si(001) substrates were cleaned in ultrasonic baths of acetone and ethanol and dried. Prior to deposition, the targets were sputter etched in pure Ar (40 sccm) for 30 sec, with shutters protecting the substrates and adjacent targets. Subsequently, the thin films were deposited in Ar atmosphere with the Ar flow set to 40 sccm, to maintain a constant total deposition pressure of 0.4 Pa. No intentional substrate heating was applied. A summary of the deposition parameters is provided in Table S1.

Surface chemistry study using XPS. Argon plasma cleaning was applied for 5 seconds which removed nearly all the physisorbed carbon impurities. The remaining carbon impurity was less than 2 at.%. Although the experiments were conducted under high vacuum ($P \sim 10^{-6} \text{ torr}$), due to the change in the vacuum conditions in long-term uses, a pristine oxide layer formation of several nanometers on the TF surface after etching was observed. Thus, the difference in intensities between the doped and undoped sample might be related to the differences in oxide layers between the doped and undoped layers, which influences the number of counts collected.

Electrochemical measurements. Electrochemical experiments were reproducible indicating that the electrode state is the same at the same potential. R_s is the intercept on the real axis, called as solution resistance (R_s), which indicates the interfacial resistance of active electrodes with hydrogen, the entire resistances of the ionic resistance of the electrolyte, and the contact resistance at the active material and current collector interface¹. Before the experiment, all solutions were re-prepared, the reference electrode was checked, and electrode contact was

cleaned to avoid high contact resistance between active material and current collector interface. Therefore, the ionic resistance of the electrolyte as well as the contact resistance of active materials can be treated as constant.

MG3 exhibits different R_s value compared that of the other electrodes, suggesting that the interfacial resistance of the thin films is somewhat higher than the others. This might be arisen from the variety in chemical composition of thin films, which was obtained by adjusting the dc power applied to the individual targets. The measured impedance from the Bode Magnitude plots (Figure S6) is reflecting the resistive behavior of this electrode, revealing high impedance magnitude value in the whole frequency range. Figure S7 depicts the Bode Phase angle dependence of PdTF and MGTFs as a function of frequency. The nature of the dominant conductive behavior of the thin films, a resistor or a capacitor, affects the real and imaginary components of the impedance and the phase angle (φ), within the system at a given frequency range. The real part of the impedance is represented as resistive behavior, and its associated phase angle is $\varphi = 0^\circ$. The imaginary part of the impedance is represented as capacitive behavior with a phase angle of $\varphi = 90^\circ$. The Bode-phase plots in different thin films modified electrodes indicate the prevailing influence of the electrolyte resistance. The films behave like ideal resistors with a very low Bode-phase angle ². As can have been shown in Figure S6, MG3 thin film shows lower phase angle than others, indicating higher resistance nature. The higher value of R_s of MG3 can be also explained by the higher roughness value of MG3 in the series causing different surface structure of film ³⁻⁵. It is obvious from the AFM images that the surfaces of MG3 thin film are rougher than others. So it is expected to have higher solution resistance for MG3. This difference suggests that the nano-structured surface roughness of the electrodes may be crucial in influencing measured values of impedance obtained for thin films.

SUPPLEMENTARY TABLES & FIGURES

Table S1. Magnetron Sputter deposition parameters of investigated films.

Batch No.	Measured Composition	Power at Pd target [W]	Power at Si target [W]	Power at Cu target [W]
Pd	Pd (crystalline)	60	-	-
MG1	Pd _{84.0} Si _{0.16.0}	65	135	-
MG2	Pd _{78.8} Si _{16.0} Cu _{5.2}	60	140	5
MG3	Pd _{74.7} Si _{16.4} Cu _{8.9}	75	125	10
MG4	Pd _{69.4} Si _{17.9} Cu _{12.7}	75	125	20
MG5	Pd _{61.8} Si _{17.9} Cu _{20.3}	60	140	20

Table S2 – XRD fitting details for the broad MG diffraction maxima and the 1st sharp Pd peak.

Sample	First Peak [°]	Remarks
Pd	40.20	Laplace Peak Function
First Broad Peak		
MG1	40.28	5 th Polynomial approximation
MG2	40.54	5 th Polynomial approximation
MG3	40.80	5 th Polynomial approximation
MG4	41.13	5 th Polynomial approximation
MG5	41.21	5 th Polynomial approximation

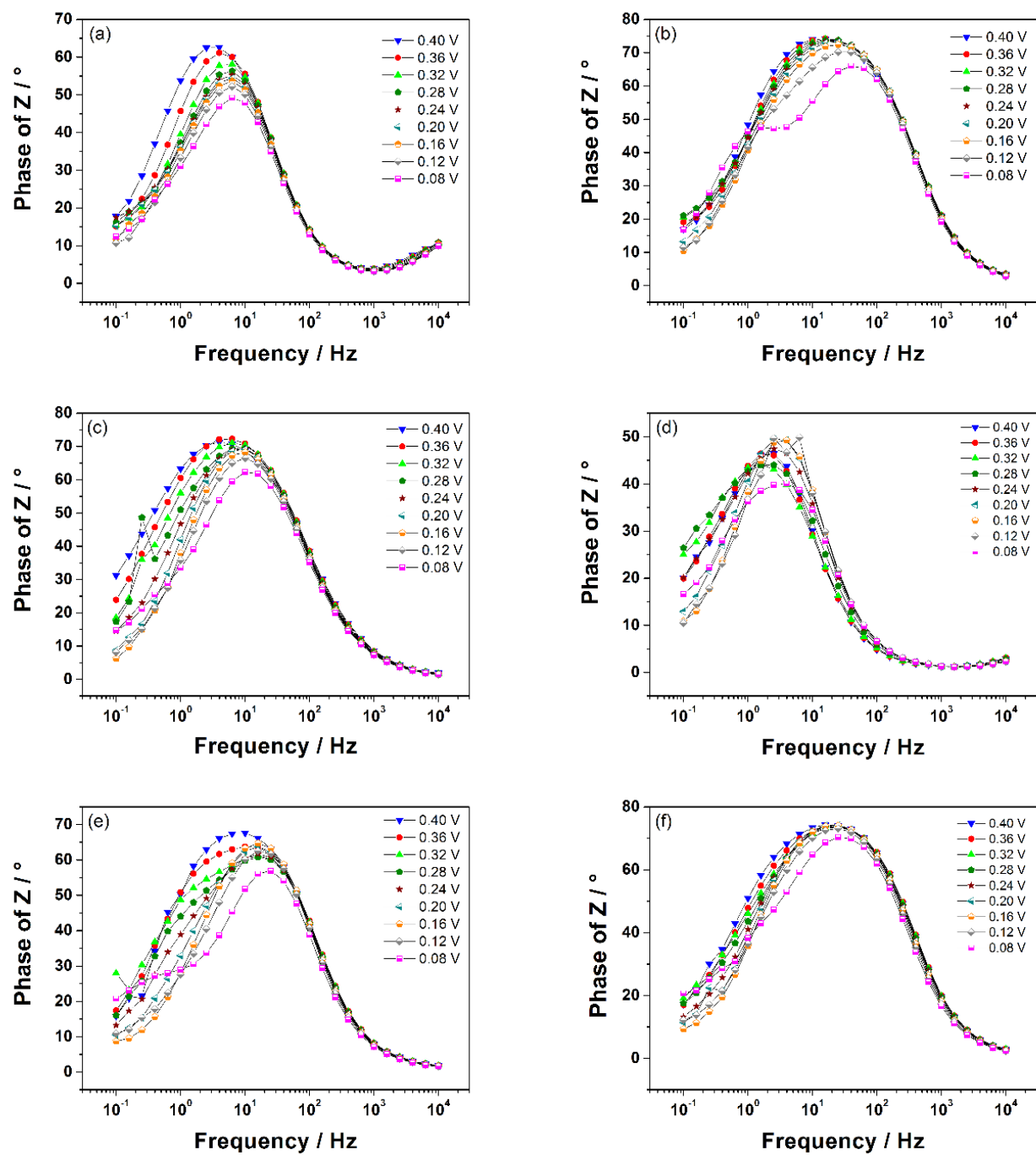


Figure S1 - Bode phase plots of (a) Pd, (b) MG1, (c) MG2, (d) MG3, (e) MG4 and (f) MG5 recorded in N_2 -saturated 0.5 M H_2SO_4 electrolyte in the potential range of 0.4 V–0.08 V.

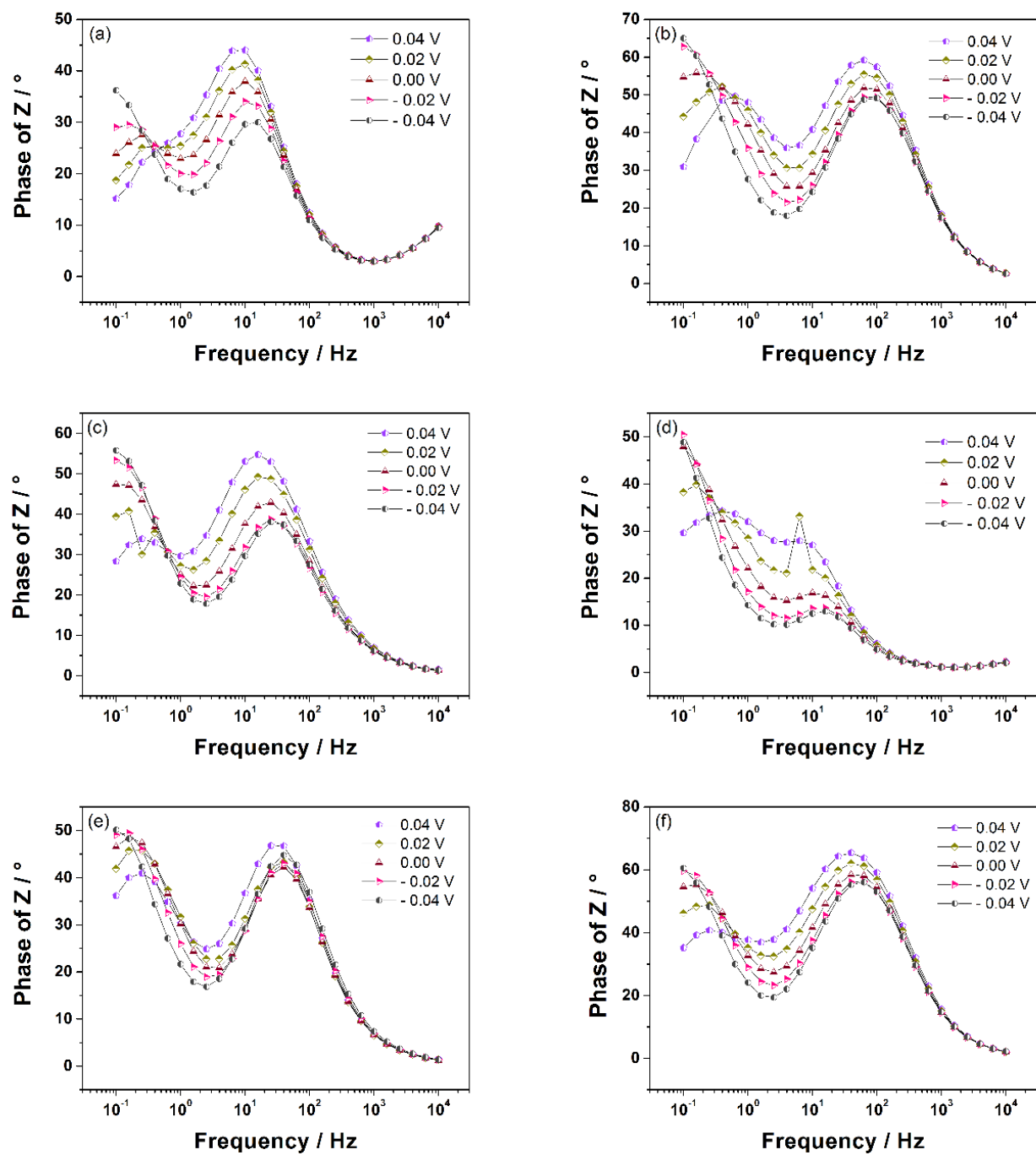


Figure S2 - Bode phase plots of (a) Pd, (b) MG1, (c) MG2, (d) MG3, (e) MG4 and (f) MG5 recorded in N_2 -saturated 0.5 M H_2SO_4 electrolyte in the potential range of 0.04 V – (-0.04) V.

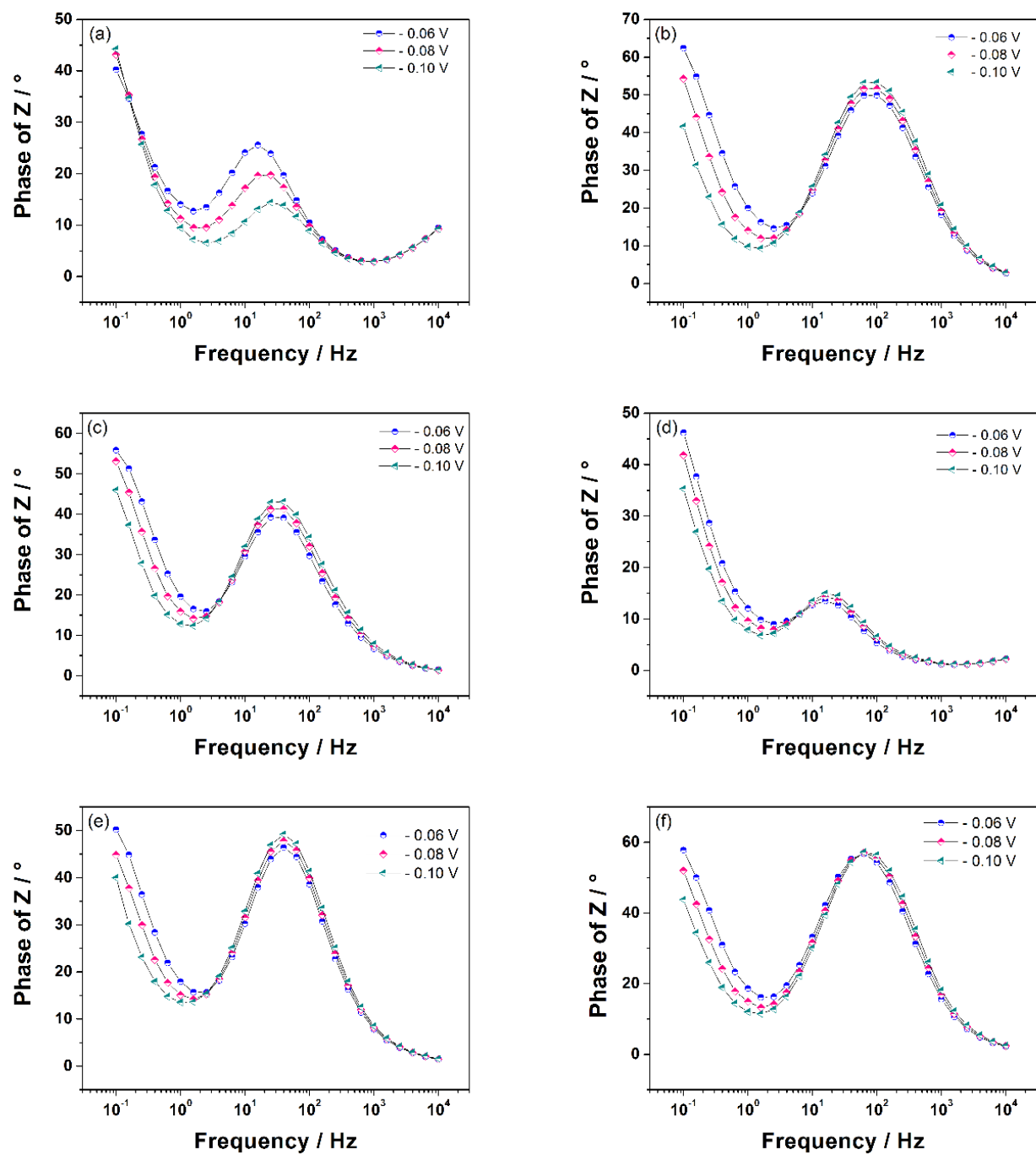


Figure S3 - Bode phase plots of (a) Pd, (b) MG1, (c) MG2, (d) MG5, (e) MG3 and (f) MG4 recorded in N_2 -saturated 0.5 M H_2SO_4 electrolyte in the potential range of (-0.06) V – (-0.1) V.

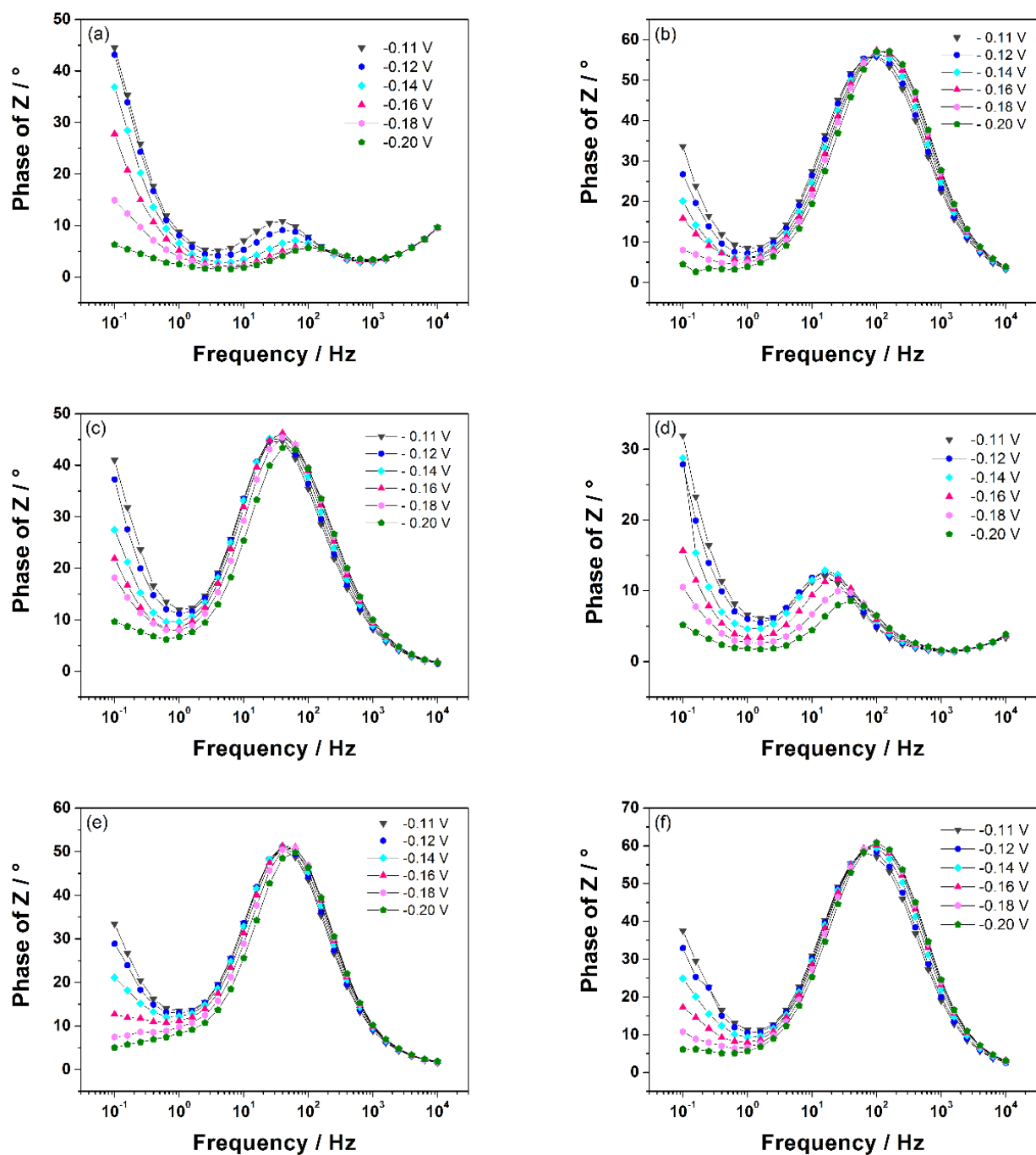


Figure S4 - Bode phase plots of (a) Pd, (b) MG1, (c) MG2, (d) MG5, (e) MG3 and (f) MG4 recorded in N_2 -saturated 0.5 M H_2SO_4 electrolyte in the potential range of (-0.11) V – (-0.2) V.

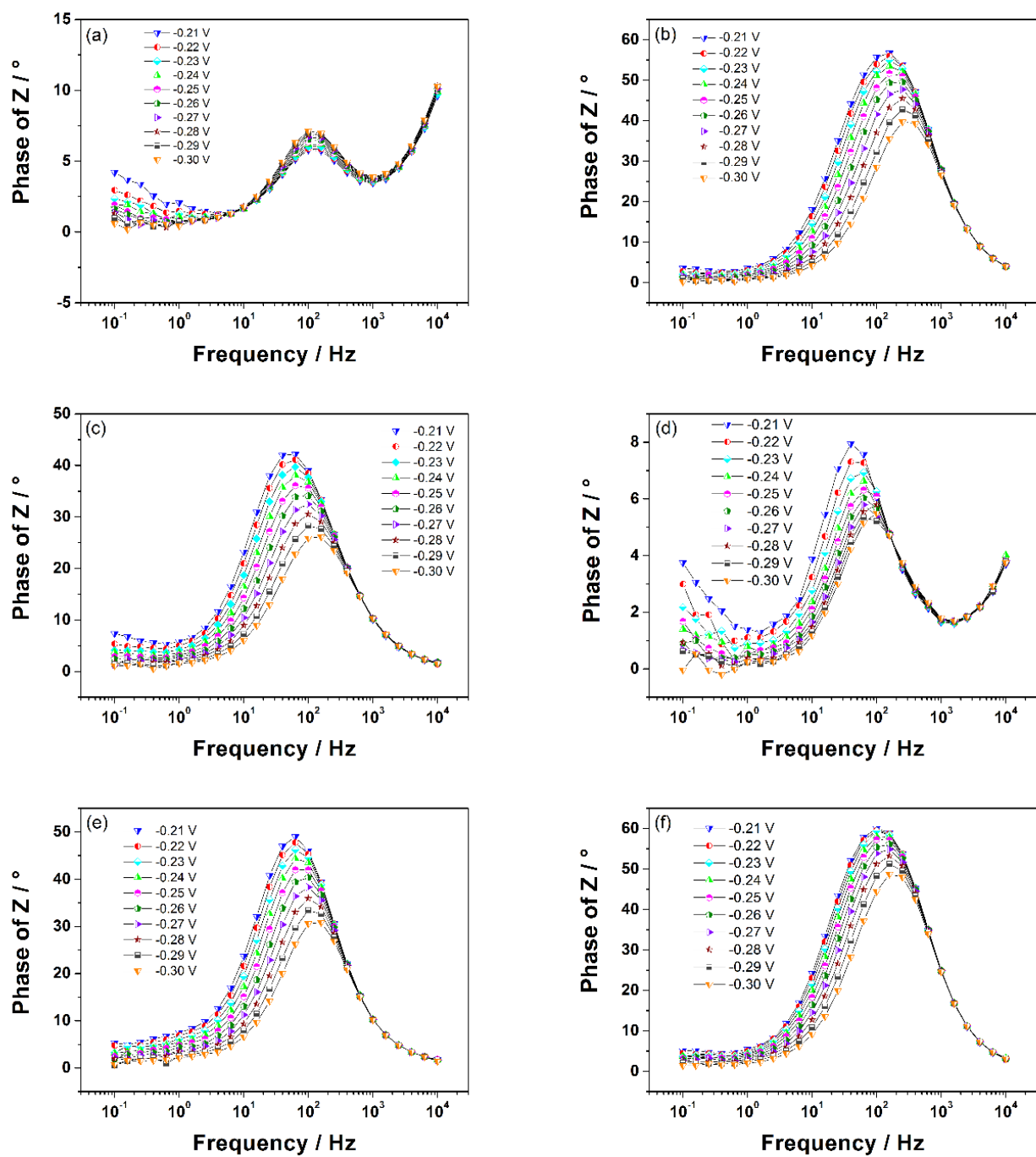


Figure S5 - Bode phase plots of (a) Pd, (b) MG1, (c) MG2, (d) MG5, (e) MG3 and (f) MG4 recorded in N_2 -saturated 0.5 M H_2SO_4 electrolyte in the potential range of (-0.21) V – (-0.3) V.

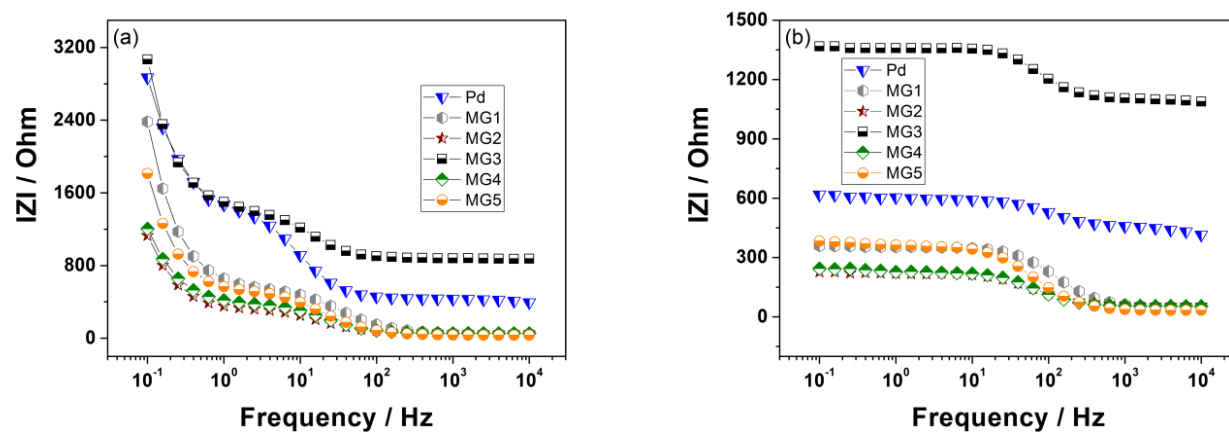


Figure S6 – Bode magnitude plots of PdTF and MGTFs at constant potentials of (a) -0.04 V and (b) -0.28 V.

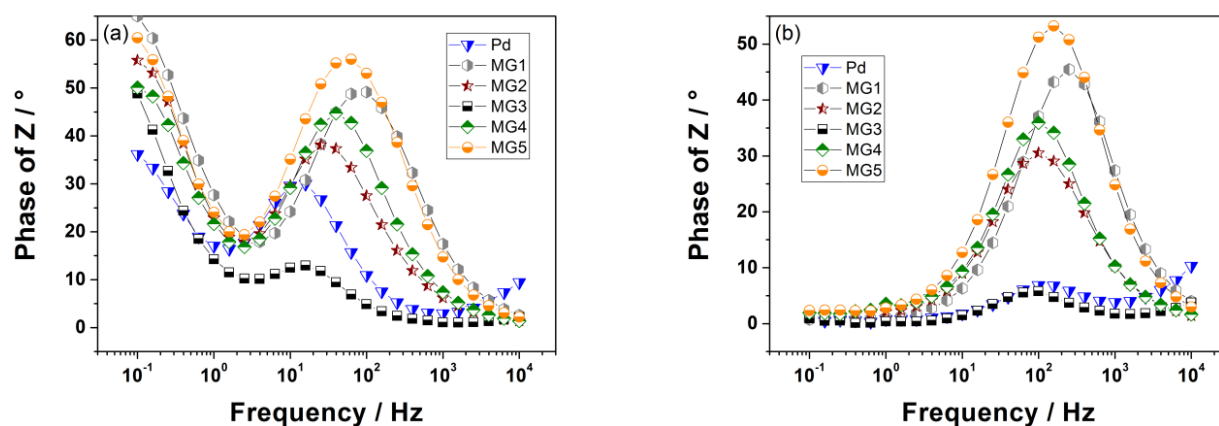


Figure S7 - Bode phase plots of PdTF and MGTFs at constant potentials of (a) -0.04 V and (b) -0.28 V.

References

1. Wang, Y. M.; Zhao, D. D.; Zhao, Y. Q.; Xu, C. L. ; Li, H. L. Effect of electrodeposition temperature on the electrochemical performance of a Ni(OH)(2) electrode. *Rsc Advances* **2012**, 2, 1074-1082.

2. Karazehir, T.;Ates, M. ;Sarac, A. S. Mott-Schottky and Morphologic Analysis of Poly(Pyrrole-N-Propionic Acid) in various electrolyte systems. *International Journal of Electrochemical Science* **2015**, *10*, 6146-6163.
3. Dagli, U.;Guler, Z. ;Sarac, A. S. Covalent Immobilization of Tyrosinase on Electrospun Polyacrylonitrile/Polyurethane/Poly(m-anthranilic acid) Nanofibers: An Electrochemical Impedance Study. *Polymer-Plastics Technology and Engineering* **2015**, *54*, 1494-1504.
4. Radecka, M.;Wierzbicka, M. ;Rekas, M. Photoelectrochemical cell studied by impedance spectroscopy. *Physica B-Condensed Matter* **2004**, *351*, 121-128.
5. Dolata, M.;Kedzierzawski, P. ;Augustynski, J. Comparative impedance spectroscopy study of rutile and anatase TiO₂ film electrodes. *Electrochimica Acta* **1996**, *41*, 1287-1293.